

Low cost and high performance Al nanoparticles for broadband light trapping in Si wafer solar cells

Yinan Zhang, Zi Ouyang, Nicholas Stokes, Baohua Jia, Zhengrong Shi et al.

Citation: *Appl. Phys. Lett.* **100**, 151101 (2012); doi: 10.1063/1.3703121

View online: <http://dx.doi.org/10.1063/1.3703121>

View Table of Contents: <http://apl.aip.org/resource/1/APPLAB/v100/i15>

Published by the [American Institute of Physics](#).

Related Articles

Light scattering at textured back contacts for n-i-p thin-film silicon solar cells

J. Appl. Phys. **111**, 083101 (2012)

Experimental analysis and computer simulation of a methodology for laser focusing in the solar cell characterization by laser beam induced current

Rev. Sci. Instrum. **83**, 043102 (2012)

Optical and electrical characteristics of asymmetric nanowire solar cells

J. Appl. Phys. **111**, 073102 (2012)

Microcrystalline silicon solar cells deposited using a plasma process excited by tailored voltage waveforms

Appl. Phys. Lett. **100**, 133504 (2012)

Integrated photonic structures for light trapping in thin-film Si solar cells

Appl. Phys. Lett. **100**, 111110 (2012)

Additional information on *Appl. Phys. Lett.*



Journal Homepage: <http://apl.aip.org/>

Journal Information: http://apl.aip.org/about/about_the_journal

Top downloads: http://apl.aip.org/features/most_downloaded

Information for Authors: <http://apl.aip.org/authors>

ADVERTISEMENT

INSTRUMENTS FOR ADVANCED SCIENCE			
	Gas Analysis dynamic measurement of reaction gas streams catalysis and thermal analysis molecular beam studies dissolved species probes fermentation, environmental and ecological studies	Surface Science UHV TPD SIMS end point detection in ion beam etch elemental imaging - surface mapping	Plasma Diagnostics plasma source characterisation etch and deposition process reaction kinetic studies analysis of neutral and radical species
	Vacuum Analysis partial pressure measurement and control of process gases reactive sputter process control vacuum diagnostics vacuum coating process monitoring		
contact Hiden Analytical for further details: info@hiden.co.uk www.HidenAnalytical.com CLICK TO VIEW OUR PRODUCT CATALOGUE			

Low cost and high performance Al nanoparticles for broadband light trapping in Si wafer solar cells

Yinan Zhang,¹ Zi Ouyang,¹ Nicholas Stokes,¹ Baohua Jia,^{1,a)} Zhengrong Shi,² and Min Gu^{1,a)}

¹Centre for Micro-Photonics, Faculty of Engineering and Industrial Sciences, Swinburne University of Technology, Hawthorn, Victoria 3122, Australia

²Suntech Power Holdings Co., Ltd., Wuxi, Jiangsu Province 214028, China

(Received 20 February 2012; accepted 26 March 2012; published online 9 April 2012)

In this paper low cost and earth abundant Al nanoparticles are simulated and compared with noble metal nanoparticles Ag and Au for plasmonic light trapping in Si wafer solar cells. It has been found tailored Al nanoparticles enable broadband light trapping leading to a 28.7% photon absorption enhancement in Si wafers, which is much larger than that induced by Ag or Au. Once combined with the SiN_x anti-reflection coating, Al nanoparticles can produce a 42.5% enhancement, which is 4.3% higher than the standard SiN_x due to the increased absorption in both the blue and near-infrared regions. © 2012 American Institute of Physics. [<http://dx.doi.org/10.1063/1.3703121>]

Metal nanoparticles supporting localized surface plasmons have attracted intensive research interests as a potentially effective way of enhancing the light absorption and thus energy conversion efficiency in solar cells.¹ Metal nanoparticles have scattering cross-sections much larger than their geometrical cross-sections, and once integrated onto the surface of solar cells, incident light would be preferentially forward scattered into the substrate.² Ag and Au nanoparticles are the most widely used materials due to their surface plasmon resonances located in the visible range and therefore interact more strongly with the peak solar intensity.^{3–8} However, such noble metal nanoparticles on the front surface of solar cells always introduce reduced light absorption in Si at the short wavelengths due to the Fano effect, i.e., the destructive interference between the scattered and unscattered light that occurs below the resonance.⁹ Moreover, the noble metal nanoparticles are impractical to implement for large-scale solar cell manufacture due to their high cost and scarcity in earth crust. The low cost and earth abundant materials Al would avoid these problems due to their surface plasmon resonance lying in the ultraviolet range, which potentially leads to a much less negative impact to the solar cell performance caused by the destructive interference effect.

In this paper, we investigated the light trapping behavior of Al nanoparticles on the front surface of Si wafer solar cells and compared with Ag and Au nanoparticles by using the finite difference time domain (FDTD) method.¹⁰ Compared to the previous studies of integrating Al nanoparticles onto the front surface of thin film solar cells,^{11–14} our investigation is of great practical significance considering the dominant status of Si wafer solar cells in the global photovoltaic industry. The insights in this paper provide a low cost and high efficiency solution for practical large-scale implementation of plasmonic nanoparticles for solar cell performance enhancement.

A spherical nanoparticle was placed on the surface of a planar semi-infinite Si slab with and without an anti-reflection coating (ARC) and illuminated under a 300–1200 nm plane wave source weighted against the air mass 1.5 solar spectrum. Perfectly matched layer boundary conditions were used in the incident direction to prevent interference effect, and periodic boundary conditions were used in the lateral direction to simulate an ordered array of nanoparticles, as shown in Fig. 1. The dielectric constants of the metal nanoparticles and Si were taken from Ref. 15 and that of SiN_x was measured by an ellipsometer from the commercial Si wafer solar cells. As a semi-infinite Si slab was used, any light travelling into the Si substrate would be absorbed. It has been confirmed these simulation conditions would only present tiny changes to the longer wavelength results when compared to the normal wafer thickness around 180 μm.

Spherical nanoparticles of a range of sizes were initially placed on the surface of the bare Si slab in an ordered

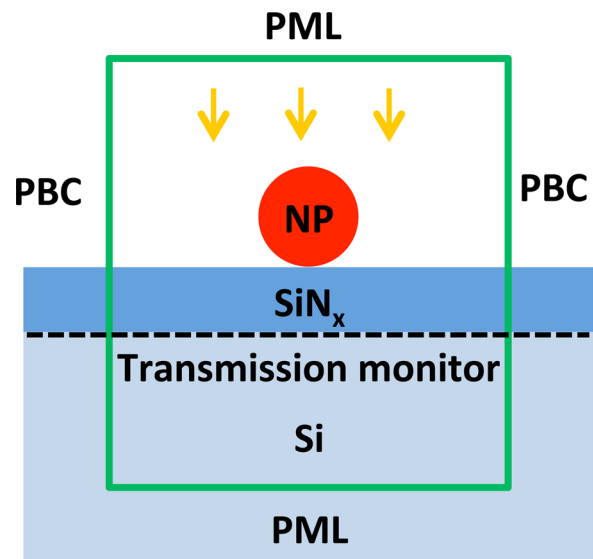


FIG. 1. Schematic of the FDTD simulation model. NP: nanoparticle; PML: perfectly matched layer; PBC: periodic boundary condition.

^{a)}Authors to whom correspondence should be addressed. Electronic addresses: bjia@swin.edu.au and mgu@swin.edu.au.

periodic array with a range of particle densities investigated. A nested parameter sweep of the nanoparticle diameter (D) was conducted in 50 nm steps from 50 to 300 nm and surface coverage (SC) ranging from 5% to 70% for each material. The best material was then similarly investigated on the surface of a SiN_x ARC at various thicknesses.

The number of photons absorbed (NPA) in the Si substrate was calculated using the following equation:

$$NPA = \frac{\int \frac{\lambda}{hc} T(\lambda) I_{AM1.5}(\lambda) d\lambda}{\int \frac{\lambda}{hc} I_{AM1.5}(\lambda) d\lambda}, \quad (1)$$

where λ is the wavelength of light in free space, h is Planck's constant, c is the speed of light in free space, $T(\lambda)$ is the transmittance of light in Si, and $I_{AM1.5}$ is the air mass 1.5 solar spectrum. The model is of high accuracy by the verification from the experimental measurement of reflectance for both the bare Si and Si with SiN_x .

The NPA as a function of parameters D and SC of the nanoparticles were investigated for all three materials compared to that of the bare Si wafer, with the resultant enhancement shown in Fig. 2. The red color identifies the enhancement in photon absorption whereas blue represents a reduction. The optimum enhancement in photon absorption for Al is 28.7% (when $D = 150$ nm and $SC = 30\%$), Ag is 27.2% ($D = 200$ nm and $SC = 20\%$), and Au is 14.5% ($D = 200$ nm and $SC = 10\%$), respectively, with stars identifying the highest enhancement in Fig. 2. In comparison, the photon absorption enhancement for a standard ARC of 75 nm SiN_x on a Si wafer is 38.2%.

A peak enhancement of NPA is clearly seen at the optimum SC and D for each material. For small nanoparticles (less than 100 nm) and large nanoparticles (larger than 200 nm), the enhancement is low. This feature is due to the light absorption by the small nanoparticles and less effective forward scattering for the large nanoparticles caused by the higher-order plasmon excitation, respectively.¹⁶ For low SC there are insufficient nanoparticles to increase the absorption to a significant level. However, for too high SC , nanoparticles start blocking significant amount of light ultimately reducing light absorption in the Si layer.

The spectral characteristics of the cells with the optimum configurations for Al, Ag, and Au nanoparticles are shown in Fig. 3 with the bare Si cell as a reference. Fig. 3(a) shows that the absorbance in the Si layer increases for all three materials, which can be attributed to the dramatically reduced light reflection, as shown in Fig. 3(b). However, the absorption in the Si for Ag and Au nanoparticles in the short wavelength region significantly reduces, compared with the bare Si cell. This phenomenon is due to the strong parasitic light absorption near the surface plasmon resonance wavelength, where more than 40% of the incident energy is dissipated around 350 and 430 nm for Ag nanoparticles and near 570 nm for Au nanoparticles, as shown in Fig. 3(c). In contrast, Al nanoparticles show broadband light absorption enhancement over the solar spectrum. This is due to the much smaller parasitic absorption in the shorter wavelength region since the surface plasmon resonance of Al nanoparticles lies in the ultraviolet region, where the intensity of solar irradiance is negligible.

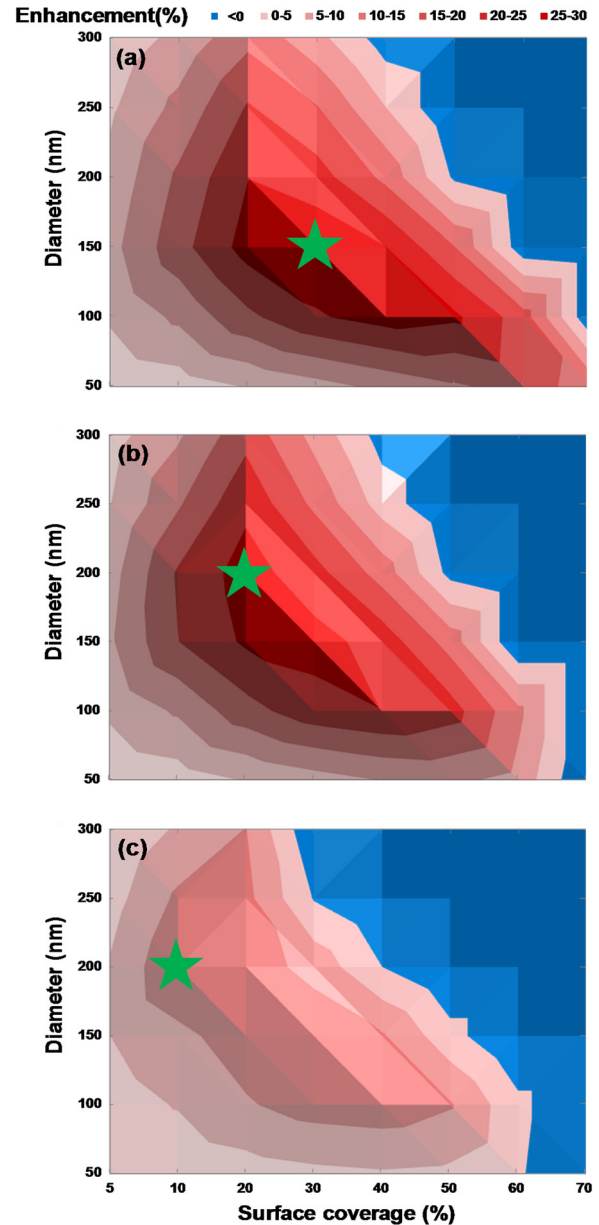


FIG. 2. Enhancement of NPA in Si as a function of parameters D and SC for (a) Al, (b) Ag, and (c) Au nanoparticles. The red color represents the enhancement whereas the blue color identifies reduction. The green star indicates the maximum enhancement.

Since Al was found to be a better material over Ag and Au in terms of light absorption enhancement in Si wafers, we expect even better photon absorption by integrating Al nanoparticles on the surface of a SiN_x ARC. As the light trapping capability of the optimized ARC and Al nanoparticles lies in different wavelength regions, the combination would lead to broader absorption enhancement. In addition to D and SC , the parameter of SiN_x thickness is introduced. To optimize the SiN_x thickness in combination with the Al nanoparticles, the NPA enhancement as a function of D and SC was constructed for each SiN_x thickness.

Fig. 4(a) shows the NPA enhancement map for the optimized SiN_x thickness of 85 nm. The peak of the NPA enhancement map is found at $D = 125$ nm and $SC = 12.5\%$ corresponding to a 42.5% enhancement as labeled with a star. It is interesting to note that for the entirety of the

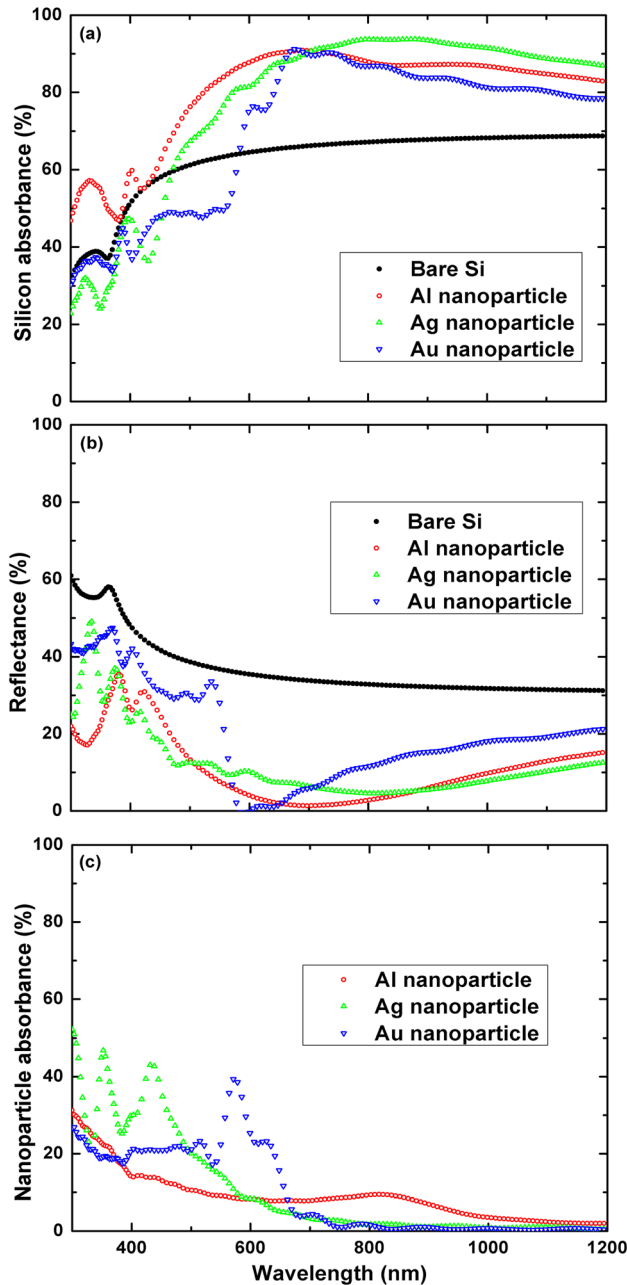


FIG. 3. Spectral characteristics of (a) Si absorbance (b) reflection (c) nanoparticle absorbance of the optimized Al (red), Ag (green), and Au (blue) nanoparticles placed on the front surface of a Si wafer compared with the bare Si.

enhancement map the lowest enhancement achieved was 38.2%, which is the same value achieved for the optimized SiN_x ARC on Si. This demonstrates that a combination of both SiN_x and Al nanoparticles can achieve a higher efficiency than the Al nanoparticles (28.7%) or the SiN_x ARC (38.2%) individually. Fig. 4(b) shows that the optimized Al nanoparticles on a 85 nm SiN_x ARC lead to higher absorbance than the standard 75 nm SiN_x ARC over almost the entire spectrum with the exception between 500 and 700 nm due to the reflection from the Al nanoparticles. The absorbance enhancement at the shorter wavelengths can be explained by the forward scattering of Al nanoparticles. The longer wavelength enhancement is due to the thicker SiN_x layer compared to the standard ARC thickness of 75 nm, which red-shifts the reflectance minimum,

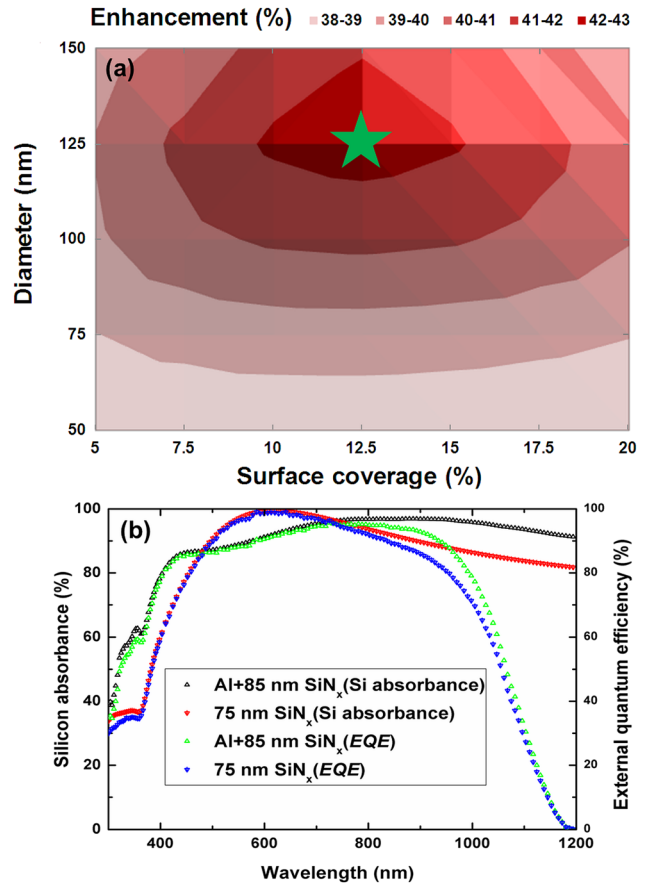


FIG. 4. (a) Enhancement of NPA for the optimized SiN_x thickness 85 nm (b) optimized Si absorbance and corresponding EQE for Al nanoparticles ($D = 125$ nm and $SC = 12.5\%$) on a 85 nm SiN_x ARC. The standard 75 nm SiN_x ARC on Si is shown for comparison.

combined with the forward scattering of the Al nanoparticles. Considering the real case that not all the photons absorbed by Si wafers would contribute to the external circuit current, we also give the external quantum efficiency (EQE) in Fig. 4(b) by using one typical internal quantum efficiency curve measured from a high efficiency solar cell. As we can see, the enhancement at shorter and longer wavelengths is still clearly observed.

It can be clearly seen that the light absorption enhancement (42.5%) in the silicon layer by integrating the Al nanoparticles is comparable to the conventional texture¹⁷⁻¹⁹ and ARC technology, which normally has an enhancement between 40% and 50%, suggesting that the proposed Al nanoparticles can be a simple and low cost alternative. Furthermore, when combining the Al nanoparticles with the standard texture and the ARC, we expect further enhancement in the silicon absorption because the enhancement mechanisms for these two light trapping strategies are different.

In conclusion, the photon absorption in a Si wafer substrate with Al nanoparticles integrated on the front surface was found to be superior to Ag and Au nanoparticles, which is due to a broadband light absorption enhancement matching the solar spectrum. Al nanoparticles in combination with the SiN_x ARC demonstrated a 4.3% higher light absorption enhancement in Si, compared with the standard SiN_x . This work provides a low cost and high efficiency solution for

practical large-scale implementation of plasmonic nanoparticles for solar cell performance enhancement.

Y.Z. would like to thank Suntech Power Holdings Co., Ltd. for providing financial support.

- ¹H. A. Atwater and A. Polman, *Nat. Mater.* **9**, 205 (2010).
- ²K. R. Catchpole and A. Polman, *Opt. Express* **16**, 21793 (2008).
- ³D. M. Schaadt, B. Feng, and E. T. Yu, *Appl. Phys. Lett.* **86**, 063106 (2005).
- ⁴S. H. Lim, W. Mar, P. Matheu, D. Derkacs, and E. T. Yu, *J. Appl. Phys.* **101**, 104309 (2007).
- ⁵S. Pillai, K. R. Catchpole, T. Trupke, and M. A. Green, *J. Appl. Phys.* **101**, 093105 (2007).
- ⁶Z. Ouyang, S. Pillai, F. Beck, O. Kunz, S. Varlamov, K. R. Catchpole, P. Campbell, and M. A. Green, *Appl. Phys. Lett.* **96**, 261109 (2010).
- ⁷P. Spinelli, M. Hebbink, R. de Waele, L. Black, F. Lenzmann, and A. Polman, *Nano Lett.* **11**, 1760 (2011).
- ⁸N. Fahim, Z. Ouyang, Y. Zhang, B. Jia, Z. Shi, and M. Gu, *Opt. Mater. Express* **2**, 190 (2012).
- ⁹J. B. Lassiter, H. Sobhani, J. A. Fan, J. Kundu, F. Capasso, P. Nordlander, and N. J. Halas, *Nano Lett.* **10**, 3184 (2010).
- ¹⁰D. M. Sullivan, in *Electromagnetic Simulation Using the FDTD Method* (IEEE, 2000).
- ¹¹A. A. Yu and W. S. Koh, *Nanotechnology* **21**, 235201 (2010).
- ¹²T. L. Temple and D. M. Bagnall, *J. Appl. Phys.* **109**, 084343 (2011).
- ¹³Y. Akimov and W. Koh, *Plasmonics* **6**, 155 (2011).
- ¹⁴L. Yang, Y. Xuan, and J. Tan, *Opt. Express* **19**, A1165 (2011).
- ¹⁵E. D. Palik, *Handbook of Optical Constants of Solids* (Elsevier, 1998).
- ¹⁶Y. A. Akimov, W. S. Koh, and K. Ostrikov, *Opt. Express* **17**, 10195 (2009).
- ¹⁷P. Campbell and M. A. Green, *J. Appl. Phys.* **62**, 243 (1987).
- ¹⁸J. H. Zhao, A. H. Wang, and M. A. Green, *Prog. Photovoltaics* **7**, 471 (1999).
- ¹⁹P. Panek, M. Lipinski, and J. Dutkiewicz, *J. Mater. Sci.* **40**, 1459 (2005).